学　位　論　文

Ectopic expression of a tight-junction molecule in podocytes is associated with childhood onset nephrotic syndrome

(ポドサイトにおけるタイト結合分子の異所性発現は小児ネフローゼ症候群に関連している)

医学研究科 (平成 25 年度入学)　小児科学分野

学籍番号　135010

菅野　修人

福島県立医科大学小児科学講座

【略語】

AR: after remission (寛解後)
BR: before remission (寛解前)
BSA: bovine serum albumin (ウシ血清アルブミン)
CLDN: Claudin (クローディン)
FSGS: focal segmental glomerulosclerosis (巣状分節性糸球体硬化症)
HSPG: Heparan Sulfate Proteoglycan (ヘパラン硫酸プロテオグリカン)
IgA-N: IgA nephritis (IgA 腎症)
mAb: monoclonal antibody (モノクローナル抗体)
MCD: minimal change disease (微小変化群)
NS: Nephrotic syndrome (ネフローゼ症候群)
pAb: polyclonal antibody (ポリクローナル抗体)
PBS: phosphate-buffered saline (リン酸緩衝生理食塩水)
PECs: parietal epithelial cells (壁側上皮細胞)
SDs: slit diaphragms (スリット膜)
TJs: tight junctions (タイト結合)

【Introduction】

Nephrotic syndrome (NS) is a complex disorder characterized by severe proteinuria along with hypoalbuminemia, edema and hyperlipidemia. The primary NS in children is most frequently caused by minimal change disease (MCD) and focal segmental glomerulosclerosis (FSGS). In both diseases, podocyte injury initiates foot process effacement, whereas the change in podocyte morphology and the resulting proteinuria are usually reversible and irreversible in MCD and FSGS, respectively. However, the pathogenesis of these diseases remains obscure, and the majority of cases cannot be explained by mutations in various podocyte genes (1, 2). In addition, it is unresolved whether MCD and FSGS are distinct types of one disease or two different diseases (3).

During early stage of glomerulogenesis, immature podocytes represent columnar epithelia with tight junctions (TJs) (4, 5, 6). On the other hand, mature podocytes lack TJs and form slit diaphragms (SDs) between opposing foot processes, establishing the final barrier to urinary protein loss. Interestingly, in several animal models for NS, TJ-like structures are generated in instead of decreased or disappeared SDs (7, 8, 9, 10). The SD-TJ transition is also observed in human MCD cases (11). Nevertheless, it is indefinite by which mechanism the SD-TJ transition occurs in both MCD and FSGS.

Claudins (CLDNs) are capable of forming TJ strands (12) and thereby the backbone of TJs. The CLDN family consists of 27 members in mammals, and shows distinct expression patterns in tissue- and cell-type specific manners (13, 14, 15, 16). Among CLDNs expressed in normal renal corpuscle, CLDN1 and CLDN2 are known to be observed in parietal epithelial cells (PECs), which cover the inner surface of Bowman's capsule, but not in podocytes (17, 18, 19). During the SD-TJ transition in MCD and FSGS, however, it is unknown which CLDN subtype is responsible for newly formed TJs in injured podocytes.

On the other hand, CLDN2 is also detected in epithelial cells of the proximal tubule and the thin descending limb of Henle along the normal renal tubule (17). CLDN2 is one of the pore-forming CLDNs, and in the proximal tubule, it has a role in the bulk reabsorption of salt and water (20). Therefore, I focused on CLDN2 and found that ectopic expression of CLDN2 existed in glomeruli of primary NS. In the present study, I show ectopic expression of CLDN2 in podocytes of pediatric MCD and FSGS. I also demonstrate that CLDN2 is associated with their pathogenesis, suggesting that both diseases are "the CLDN2-related podocytopathies". Moreover, I discuss the possible mechanism by which CLDN2 expression in podocytes lead to their dysfunction.

【Methods】

Patients

Renal frozen specimens were obtained by needle biopsy from 49 pediatric patients: 21 subjects (8 subjects before remission [BR] and 13 after remission [AR]) with MCD, 18 (8 BR and 10 AR) with FSGS, and 10 with IgA nephritis (IgA-N) as disease controls. This study was approved by the Ethical Committee of Fukushima Medical University (approval number: 1809).

Clinical data for the subjects were documented at the time of biopsy, and were summarized in Tables 1 and 2. Proteinuria and urinary occult blood were semi-quantitatively scored as follows: (−)=0, (±)=0.5, (1+)=1, (2+)=2, (3+)=3, and (4+)=4.

Antibodies

Rabbit polyclonal antibody (pAb) against CLDN2 was the gift from Dr. Furuse (National Institute for Physiological Sciences, National Institutes of Natural Sciences) (21). Rabbit pAbs against CLDN1 and podocin were purchased from IBL (Gunma, Japan) and SIGMA (St. Louis, MO, USA), respectively. Mouse monoclonal antibodies (mAbs) against CD34 (clone NU-4A1), podocalyxin (clone #222328) and synaptopodin (clone G1D4) were obtained from Nichirei Bioscience (Tokyo, Japan), R&D Systems (Minneapolis, MN, USA) and Progen Biotechnik (Heidelberg Germany), respectively. A rat anti-Heparan Sulfate Proteoglycan (HSPG) (Perlecan) mAb (clone A7L6) was purchased from Merck Millipore (Temecula, CA, USA). The secondary antibodies used were as follows: AlexaFluor488-labeled donkey anti-rabbit IgG (H+L) (Invitrogen, Waltham, MA, USA), Cy3-conjugated AffiniPure donkey anti-mouse IgG (H+L) (Jackson ImmunoResearch, West Grove, PA, USA), AlexaFluor647-labeled AffiniPure donkey anti-rat IgG (H+L) (Jackson ImmunoResearch) and immunogold conjugate EM goat anti-rabbit IgG (BBI Solutions, Cardiff, UK).

Immunohistochemistry

Renal biopsy specimens were frozen on dry ice and kept at −80°C until use. They were sectioned at a thickness of 5 μm and fixed in ice-cold methanol for 15 min at −20°C. After washing with phosphate-buffered saline (PBS), sections were blocked in 2% bovine serum albumin (BSA) for 1 h at room temperature. After washing, they were subsequently incubated with primary antibodies overnight at 4°C and rinsed again with PBS followed by a reaction for 1 h at room temperature with appropriate secondary antibodies. They were then mounted after washing with PBS. All samples were

examined using a laser-scanning confocal microscopy (FV1000, OLYMPUS, Tokyo, Japan).

Calculations

The CLDN2-positive area was calculated using image processing software (ImageJ, Java). The images stained with CLDN2 and HSPG (Perlecan) were set the threshold from 100 to 255, in order to exclude background signals. A circle was drawn by free hand along the inside of PECs, and the total area in the circle (A) and the CLDN2-expression area in the circle (B) were determined. The CLDN2-positive area was defined as B/A × 100 (%), and represented using box-and-whisker plots.

Immunoelectron microscopy

Renal biopsy tissues were fixed with periodate-lysine-paraformaldehyde for 2 h at 4°C, and, after washing with PBS, they were incubated with polyvinylpyrrolidone-sucrose overnight at 4°C. They were then frozen by liquid nitrogen and ultrathin cryosections were prepared using a Leica Ultracut UCT microtome equipped with the FCS cryoattachment (Wien, Austria) at –20°C. They were transferred to nickel grids (150 mesh) with coating in formvar and carbon, and subsequent incubation steps were carried out by floating grids on droplets of the filtered soluction. After quenching free aldehyde groups with PBS/0.01 M glycine, sections were incubated with rabbit anti-CLDN2 pAb overnight at 4°C, and reacted for 1 h at room temperature with 10 nm gold-labeled goat anti-rabbit IgG followed by a fixation with 2.5% glutaraldehyde buffered with 0.1 M PBS (pH 7.4). They were subsequently contrasted with 3% uranyl acetate solution for 40 min, and absorption-stained with 3% polyvinyl alcohol containing 0.2% acidic uranyl acetate for 40 min. Micrographs were captured using an electron microscope (JEM1230, JOEL).

Statistical analysis

All values are shown as the mean ± standard deviation (SD) except for those of the CLDN2-positive area. Statistical analysis was performed by IBM SPSS statistics 23 software (Chicago, IL, USA). Results were analyzed using two-sample *t*-test and one way analysis of variance (ANOVA).

【Results】

CLDN2 is ectopically detected in MCD and FSGS glomeruli

I first examined, by immunohistochemistry, the expression of CLDN2 in glomeruli obtained from pediatric MCD and FSGS patients, as well as in those from IgA-N subjects as disease controls. To distinguish the overall structure of glomeruli, the endothelial marker CD34 and the basement membrane marker HSPG (Perlecan) were co-immunostained with CLDN2. As shown in Figure 1, strong filamentous signals for CLDN2 appeared to be detected in the before remission cases with MCD and FSGS, but not in subjects with IgA-N. CLDN2 was also occasionally observed within whole cell bodies. These CLDN2 signals were generally distributed close to the basement membrane and separated from endothelial cells, implying that CLDN2-expressing cells correspond to podocytes. By contrast, in the after remission cases with the MCD and FSGS, the CLDN2 expression was strikingly decreased, and the filamentous and cytoplasmic staining disappeared.

I also quantitatively evaluated the CLDN2 expression by calculating the positive area in glomeruli (Figure 2). The CLDN2-stained region in MCD and FSGS glomeruli before remission was significantly greater than that after remission and in IgA-N patients. In addition, the abundance of CLDN2 expression was well correlated with the amounts of proteinuria of each group at the time of biopsy (Table 1 and 2). Interestingly, among before remission subjects, CLDN2 was expressed in MCD glomeruli at high levels compared with that in FSGS.

CLDN2 is expressed in MCD and FSGS podocytes

To determine whether CLDN2-expressing cells represent podocytes, I next performed multiple immunostaining using the podocyte markers synaptopodin (SYNPO) and podocalyxin (PODXL) (22, 23) (Figure 3). In both MCD and FSGS glomeruli before remission, CLDN2 was at least in part colocalized with SYNPO and PODXL, suggesting that CLDN2 expression is observed in podocytes.

I subsequently verified, by immunogold immunoelectron microscopy, the nature of CLDN2-positve cells in MCD glomeruli before remission, as well as the detailed subcellular localization of CLDN2 (Figure 4). The CLDN2 labeling was detected not only in residual foot processes of podocytes (Figure 4A) but also in fused foot processes (Figure 4B). Importantly, CLDN2 was also concentrated along newly formed TJs in podocytes (Figure 4C).

CLDN1 is not expressed in MCD glomeruli but segmentally observed in FSGS

I also evaluated the CLDN1 expression in renal corpuscle of MCD and FSGS cases before remission (Figure 5). As expected, PECs were positive for CLDN1 in both diseases. By contrast, in glomeruli, the CLDN1 signals were not apparently detected for MCD subjects. In addition, CLDN1 was only focally and segmentally expressed in FSGS glomeruli with a trabecular pattern.

Newly formed TJs constructed by CLDN2 are generated together with decrease of SDs in MCD and FSGS glomeruli before remission

To confirm the SD-TJ transition, I performed multiple immunostaining using the SDs marker podocin (24), and compared CLDN2 and podocin expression in MCD and FSGS glomeruli (Figure 6). In the before remission cases with MCD and FSGS, the filamentous signals for podocin were decreased and changed to the granulated signals together with the expression of strong filamentous signals for CLDN2. By contrast, in the after remission cases with MCD and FSGS, the filamentous signals for podocin were recovered together with decreased expression for CLDN2.

【Discussion】

In the present study, I found that CLDN2, which is detected in epithelial cells of Bowman's capsule, the proximal tubule and the thin descending limb of Henle along the normal nephron (17), was ectopically expressed on injured podocytes in pediatric MCD and FSGS. In both diseases, CLDN2 was distributed along the glomerular basement membrane maker HSPG, and apart from the vascular endothelial marker CD34. In addition, CLDN2 was at least in part colocalized with the podocyte markers SYNPO and PODXL in MCD and FSGS. Moreover, CLDN2-immunogold signals was observed in podocytes, especially in residual and fused foot processes as well as at TJs, definitively indicating that CLDN2-expressing cells represent podocytes. Hence, immunofluorescence and immunoelectron studies for CLDN2 appear to be a powerful tool for diagnosis of these primary NS. Since no substantial abnormality in glomerular structure is detected in MCD by light microcopy, CLDN2 should be a novel diagnostic marker especially for these patients who are resistant to steroid therapy and underwent renal biopsy (25).

Although both MCD and FSGS are typical podocyte diseases (26, 27), information on the pathophysiological basis for these diseases is still fragmentary. In this regard, it is noteworthy that ectopic expression of CLDN2 on podocytes was observed not only in MCD but also in FSGS as far as we determined. Thus, both MCD and FSGS could be regarded as "the CLDN2-related podocytopathies". Lower expression levels of CLDN2 in FSGS before remission compared with that in MCD most probably reflect podocyte loss in FSGS. The CLDN2-immunoreactive area in podocytes of both diseases after remission was significantly decreased to levels similar to that of the disease control group, further supporting that the CLDN2 expression is involved in their pathogenesis. Since circulating glomerular permeability factors, including angiopoietin-like-4 and urokinase plasminogen activator receptor in MCD and FSGS, respectively, are expected to result in the onset of these diseases (3, 28, 29, 30), it is intriguing to elucidate whether and how these factors are associated with the CLDN2 expression in damaged podocytes.

The CLDN1 expression, which is restricted in PECs along the healthy nephron (17, 18), is induced in glomerulus from humans and animals with diabetic nephropathy (31). On the other hand, we demonstrated that CLDN1 was not principally observed in glomerular tuft of pediatric MCD. In FSGS glomeruli before remission, the CLDN1 signals displayed a cord-like array in focal and segmental patterns, which are totally different from those of CLDN2. In FSGS, PECs are activated on Bowman's capsule and migrate onto the glomerular capillary to substitute or dislocate podocytes (32).

Activated PECs in glomerulosclerotic lesions are also known to positive for CLDN1 (33). Taken collectively, CLDN1-expressing cells in glomeruli of our FSCG cases may correspond to activated PECs.

Podocin is one of the proteins forming SDs, and its mutations (NPHS2 gene) are responsible for the autosomal recessive form of steroid-resistant NS (24). The strong filamentous signals for CLDN2 were appeared together with decrease of the filamentous signals and change to the granulated pattern for podocin in the before remission cases with MCD and FSGS. These changes are suggested that SDs are displaced to TJs constructed by CLDN2 in the before remission cases of MCD and FSGS. In the after remission cases with MCD and FSGS, the filamentous signals for podocin were recovered. It is seemed that the SDs related molecules containing podocin accumulate and form SDs again.

Several TJ proteins such as junctional adhesion molecule-A, coxsackie and adenovirus receptor, ZO-1 and cingulin, are concentrated at the SD in mature podocytes (34, 35, 36). Among them, ZO-1 is indispensable for the interdigitation of foot processes and the formation of SDs (37), even though the precise role of other TJ components in glomerular filtration barrier remains elusive. Therefore, I speculate that the ectopically expressed CLDN2 could recruit these TJ constituents from the SD pool and disrupt the architecture of foot processes and SDs, resulting in being dedifferentiated into immature podocytes with glomerular dysfunction. To prove this idea, CLDN2-knockin mice, in which CLDN2 is podocyte-specifically expressed under human podocin promoter, were generated, and their characterization is under analysis (Ichikawa-Tomikawa et al., unpublished data).

In conclusion, I showed that both MCD and FSGS in children possessed the same pathological findings in terms of ectopic CLDN2 expression on podocytes. I also demonstrated that the abundance of CLDN2 was diminished after remission, indicating that the levels of CLDN2 expression are related to the disease state. Further studies are required to clarify the functional relevance of CLDN2 expression in the pathogenesis of these diseases.

【Acknowledgments】

I thank Prof. M Hosoya, assistant Prof. Y Kawasaki, and Prof. H Chiba (Fukushima Medical University) for their advice. I am also grateful to Drs. N Ichikawa-Tomikawa and M Mizuko (Fukushima Medical University) for immunohistochemical study; Dr. K Sugimoto (Fukushima Medical University) for preparing figures; and Dr. H Kurihara (Juntendo University) for immunoelectron microscopy analysis.

【References】

1. Allison A Eddy, Jordan M Symons: Nephrotic syndrome in childhood. Lancet 362: 629-639, 2003

2. D'Agati VD, Kaskel FJ, Falk RJ: Focal segmental glomerulosclerosis. N Engl J Med. 365: 2398-2411, 2011

3. Floege J, Amann K: Primary glomerulonephritides. Lancet 387: 2036-2048, 2016

4. Reeves W, Caulfield JP, Farquhar MG: Differentiation of epithelial foot processes and filtration slits: sequential appearance of occluding junctions, epithelial polyanion, and slit membranes in developing glomeruli. Lab Invest. 39: 90-100, 1978

5. Grahammer F, Schell C, Huber TB: The podocyte slit diaphragm—from a thin grey line to a complex signalling hub. Nat Rev Nephrol. 9: 587-598, 2013

6. Schell C, Wanner N, Huber TB: Glomerular development—shaping the multi-cellular filtration unit. Semin Cell Dev Biol. 36: 39-49, 2014

7. Pricam C, Humbert F, Perrelet A, Amherdt M, Orci L: Intercellular junctions in podocytes of the nephrotic glomerulus as seen with freeze-fracture. Lab Invest. 33: 209-218, 1975

8. Ryan GB, Leventhal M, Karnovsky MJ: A freeze-fracture study of the junctions between glomerular epithelial cells in aminonucleoside nephrosis. Lab Invest. 32: 397-403, 1975

9. Caulfield JP, Reid JJ, Farquhar MG: Alterations of the glomerular epithelium in acute aminonucleoside nephrosis. Evidence for formation of occluding junctions and epithelial cell detachment. Lab Invest. 34: 43-59, 1976

10. Kurihara H, Anderson JM, Kerjaschki D, Farquhar MG: The altered glomerular filtration slits seen in puromycin aminonucleoside nephrosis and protamine sulfate-treated rats contain the tight junction protein ZO-1. Am J Pathol. 141: 805-816, 1992

11. Lahdenkari AT, Lounatmaa K, Patrakka J, Holmberg C, Wartiovaara J, Kestilä M, Koskimies O, Jalanko H: Podocytes are firmly attached to glomerular basement membrane in kidneys with heavy proteinuria. J Am Soc Nephrol. 15: 2611-2618, 2004

12. Furuse M, Sasaki H, Fujimoto K, Tsukita S. A single gene product, claudin-1 or -2, reconstitutes tight junction strands and recruits occludin in fibroblasts. J Cell Biol.143: 391–401, 1998

13. Tsukita S, Furuse M, Itoh M. Multifunctional strands in tight junctions. Nat Rev Mol Cell Biol. 2: 285–293, 2001

14. Van Itallie CM, Anderson JM: Claudins and epithelial paracellular transport. Annu Rev Physiol. 68: 403-429, 2006

15. Chiba H, Osanai M, Murata M, Kojima T, Sawada N: Transmembrane proteins of tight junctions. Biochim Biophys Acta. 1778: 588-600, 2008

16. Günzel D, Yu AS: Claudins and the modulation of tight junction permeability. Physiol Rev. 93: 525-569, 2013

17. Kiuchi-Saishin Y, Gotoh S, Furuse M, Takasuga A, Tano Y, Tsukita S: Differential expression patterns of claudins, tight junction membrane proteins, in mouse nephron segments. J Am Soc Nephrol. 13: 875-886, 2002

18. Ohse T, Pippin JW, Vaughan MR, Brinkkoetter PT, Krofft RD, Shankland SJ: Establishment of conditionally immortalized mouse glomerular parietal epithelial cells in culture. J Am Soc Nephrol. 19: 1879-1890, 2008

19. Ohse T, Pippin JW, Chang AM, Krofft RD, Miner JH, Vaughan MR, Shankland SJ: The enigmatic parietal epithelial cell is finally getting noticed: a review. Kidney Int. 76: 1225-1238, 2009

20. Yu AS: Claudins and the kidney. J Am Soc Nephrol. 26: 11-19, 2015

21. Kubota K, Furuse M, Sasaki H, Sonoda N, Fujita K, Nagafuchi A, Tsukita S: Ca^{2+}-independent cell-adhesion activity of claudins, a family of integral membrane proteins localized at tight junctions. Curr Biol. 9: 1035-1038, 1999

22. Kerjaschki D, Sharkey DJ, Farquhar MG: Identification and characterization of podocalyxin—the major sialoprotein of the renal glomerular epithelial cell. J Cell Biol. 98: 1591-1596, 1984

23. Mundel P, Heid HW, Mundel TM, Krüger M, Reiser J, Kriz W: Synaptopodin: an actin-associated protein in telencephalic dendrites and renal podocytes. J Cell Biol. 139: 193-204, 1997

24. Caridi G, Bertelli R, Carrea A, Di Duca M, Catarsi P, Artero M, Carraro M, Zennaro C, Candiano G, Musante L, Seri M, Ginevri F, Perfumo F, Ghiggeri GM: Prevalence, genetics, and clinical features of patients carrying podocin mutations in steroid-resistant nonfamilial focal segmental glomerulosclerosis. J Am Soc Nephrol. 12: 2742-2746, 2001

25. Gulati S, Sharma AP, Sharma RK, Gupta A, Gupta RK: Do current recommendations for kidney biopsy in nephrotic syndrome need modifications? Pediatr Nephrol. 17: 404-408, 2002

26. Wiggins RC: The spectrum of podocytopathies: a unifying view of glomerular diseases. Kidney Int. 71: 1205-1214, 2007

27. D'Agati VD: The spectrum of focal segmental glomerulosclerosis: new insights. Curr Opin Nephrol Hypertens. 17: 271-281, 2008

28. Clement LC, Avila-Casado C, Macé C, Soria E, Bakker WW, Kersten S, Chugh SS: Podocyte-secreted angiopoietin-like-4 mediates proteinuria in glucocorticoid-sensitive nephrotic syndrome. Nat Med. 17: 117-122, 2011

29. Wei C, El Hindi S, Li J, Fornoni A, Goes N, Sageshima J, Maiguel D, Karumanchi SA, Yap HK, Saleem M, Zhang Q, Nikolic B, Chaudhuri A, Daftarian P, Salido E, Torres A, Salifu M, Sarwal MM, Schaefer F, Morath C, Schwenger V, Zeier M, Gupta V, Roth D, Rastaldi MP, Burke G, Ruiz P, Reiser J: Circulating urokinase

receptor as a cause of focal segmental glomerulosclerosis. Nat Med. 17: 952-960, 2011

30. Chugh SS, Clement LC, Macé C: New insights into human minimal change disease: lessons from animal models. Am J Kidney Dis. 59: 284-292, 2012

31. Hasegawa K, Wakino S, Simic P, Sakamaki Y, Minakuchi H, Fujimura K, Hosoya K, Komatsu M, Kaneko Y, Kanda T, Kubota E, Tokuyama H, Hayashi K, Guarente L, Itoh H: Renal tubular Sirt1 attenuates diabetic albuminuria by epigenetically suppressing Claudin-1 overexpression in podocytes. Nat Med. 19: 1496-1504, 2013

32. Shankland SJ, Smeets B, Pippin JW, Moeller MJ: The emergence of the glomerular parietal epithelial cell. Nat Rev Nephrol. 10: 158-173, 2014

33. Smeets B, Kuppe C, Sicking EM, Fuss A, Jirak P, van Kuppevelt TH, Endlich K, Wetzels JF, Gröne HJ, Floege J, Moeller MJ: Parietal epithelial cells participate in the formation of sclerotic lesions in focal segmental glomerulosclerosis. J Am Soc Nephrol. 22: 1262-1274, 2011

34. Schnabel E, Anderson JM, Farquhar MG: The tight junction protein ZO-1 is concentrated along slit diaphragms of the glomerular epithelium. J Cell Biol. 111: 1255-1263, 1990

35. Nagai M, Yaoita E, Yoshida Y, Kuwano R, Nameta M, Ohshiro K, Isome M, Fujinaka H, Suzuki S, Suzuki J, Suzuki H, Yamamoto T: Coxsackievirus and adenovirus receptor, a tight junction membrane protein, is expressed in glomerular podocytes in the kidney. Lab Invest. 83: 901-911, 2003

36. Fukasawa H, Bornheimer S, Kudlicka K, Farquhar MG: Slit diaphragms contain tight junction proteins. J Am Soc Nephrol. 20: 1491-1503, 2009

37. Itoh M, Nakadate K, Horibata Y, Matsusaka T, Xu J, Hunziker W, Sugimoto H: The structural and functional organization of the podocyte filtration slits is regulated by Tjp1/ZO-1. PLoS One 9: e106621, 2014

Table 1: Clinical characteristics of patients in this study.

	MCD	FSGS	*p* value[a]	IgA-N	*p* value[b]
Total number of patients	**21**	**18**		**10**	
Age at onset	**5.38±3.78**	**6.00±3.74**	**0.61**	**11.40±2.88**	**<0.01**
Age at biopsy	**7.05±4.01**	**8.17±4.69**	**0.43**	**12.80±2.90**	**<0.01**
Sex (male) (%)	**12 (57%)**	**16 (89%)**		**7 (70%)**	
Proteinuria (maximum)					
Urinary protein score	**3.50±0.95**	**3.75±0.45**	**0.31**	**1.50±1.05**	**<0.01**
Proteinuria (g/day)	**4.49±4.13**	**10.17±6.46**	**<0.01**	**0.49±0.81**	**<0.01**
Urine occult blood score	**0.21±0.68**	**0.39±0.96**	**0.51**	**1.95±1.12**	**<0.01**
Serum creatinine (mg/dl)	**0.32±0.09**	**0.44±0.21**	**<0.05**	**0.54±0.14**	**<0.01**

The values represent the mean ±SD.

[a, b]: Two-sample *t*-test.

[a]: *p* value compared the values in the MCD group with those in the FSGS group.

[b]: *p* value compared the values in the MCD group with those in the IgA-N group.

Table 2: Comparison of clinical characteristics between the before and after remission cases in patients with MCD and FSGS.

	MCD			FSGS		
	BR	**AR**	***p* value[a]**	**BR**	**AR**	***p* value[b]**
Total number of patients	**8**	**13**		**8**	**10**	
Age at onset	**7.50±4.24**	**4.07±2.91**	**<0.05**	**6.25±3.58**	**5.80±4.05**	**0.81**
Age at biopsy	**7.63±4.10**	**6.69±4.07**	**0.62**	**6.88±3.80**	**9.20±5.27**	**0.31**
Sex (male) (%)	**2 (25%)**	**10 (77%)**		**6 (75%)**	**10 (100%)**	
Proteinuria						
(At the time of biopsy)						
Urinary protein score	**2.75±1.04**	**0.04±0.14**	**<0.01**	**2.81±1.46**	**0.00±0.00**	**<0.01**
Proteinuria (g/day)	**2.14±1.46**	**0.01±0.03**	**<0.01**	**1.88±1.47**	**0.00±0.01**	**<0.01**
(maximum)						
Urinary protein score	**3.50±0.93**	**3.50±1.00**	**1.00**	**3.75±0.46**	**3.75±0.46**	**1.00**
Proteinuria (g/day)	**4.06±2.31**	**4.77±5.08**	**0.72**	**7.79±7.13**	**12.88±4.68**	**0.13**
Urine occult blood score	**0.56±1.05**	**0.00±0.00**	**0.17**	**0.81±1.36**	**0.05±0.16**	**0.16**
Serum creatinine (mg/dl)	**0.33±0.12**	**0.32±0.08**	**0.87**	**0.38±0.22**	**0.49±0.20**	**0.30**

BR: before remission, AR: after remission. The values represent the mean ±SD.

[a, b]: Two-sample *t*-test.

[a]: *p* value compared the values in the BR group with those in the AR group of MCD.

[b]: *p* value compared the values in the BR group with those in the AR group of FSGS.

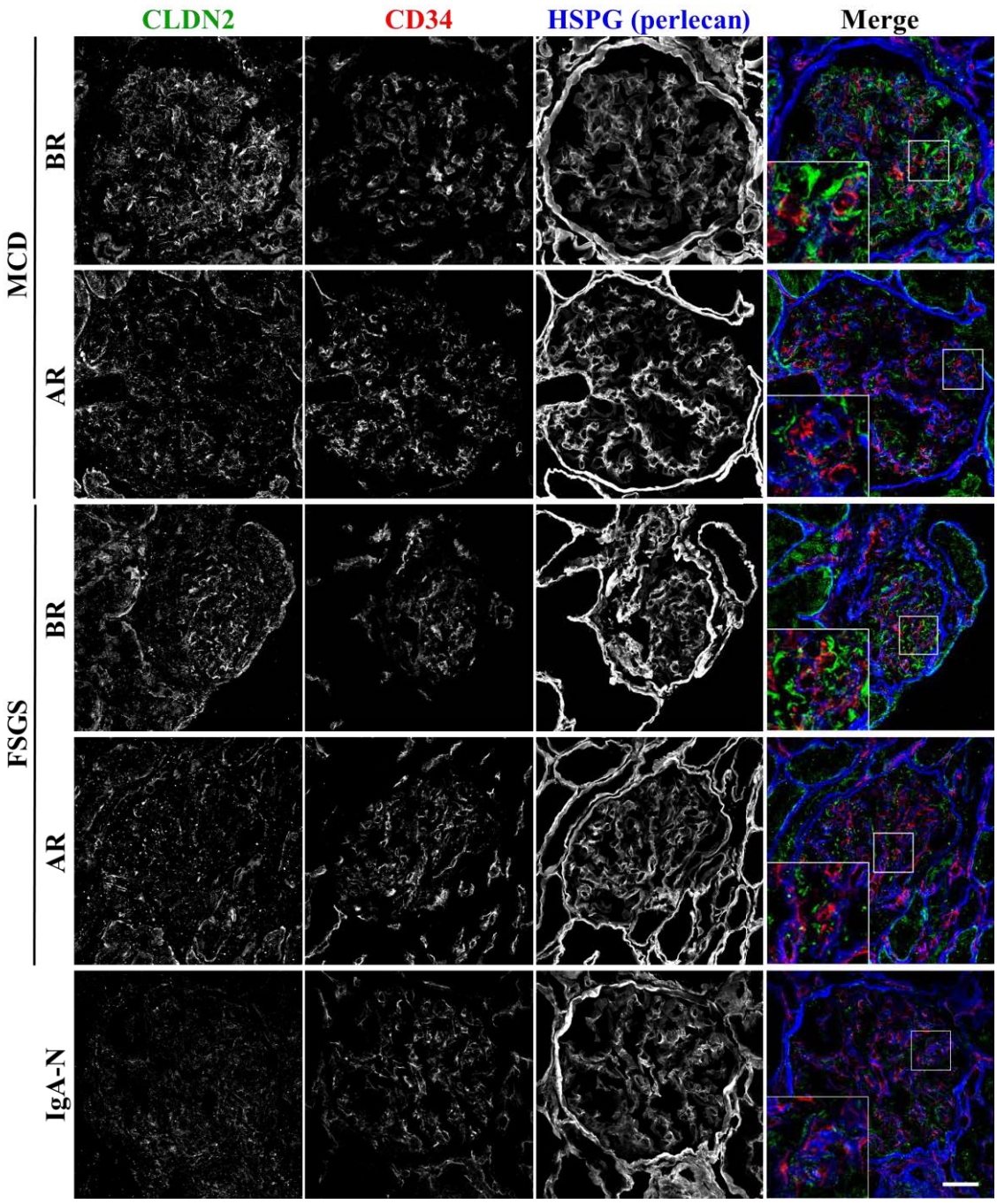

Figure 1: CLDN2 is ectopically expressed in MCD and FSGS glomeruli.

Renal biopsy sections were subjected to immunostaining with the corresponding antibodies. Typical micrographs are shown for the before remission (BR) and after remission (AR) cases in MCD and FSGS, as well as the case in IgA-N. In the Merge panels, CLDN2 is stained green, CD34 is red and HSPG (perlecan) is blue. Bar, 50 μm.

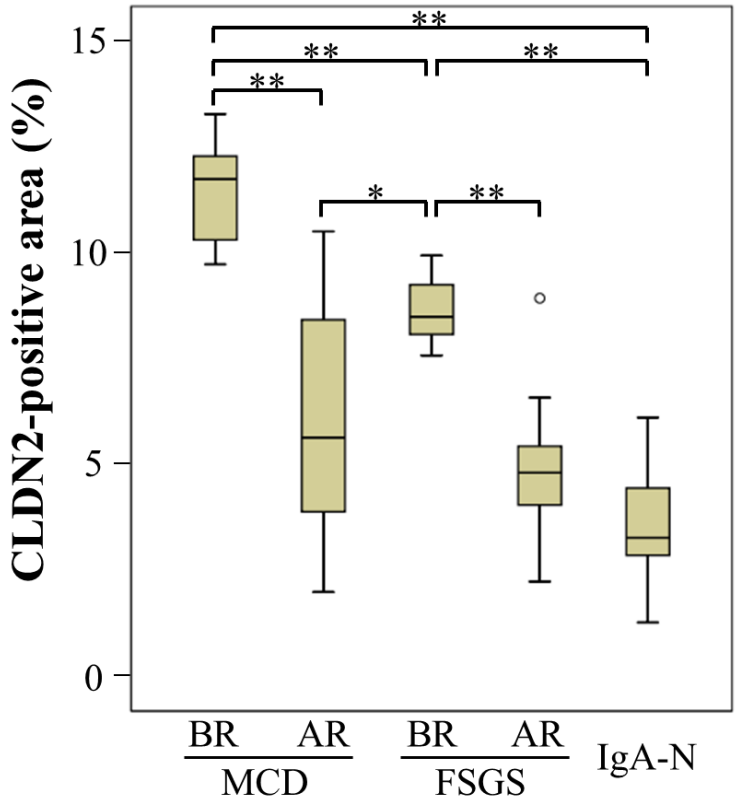

Figure 2: The CLDN2-positive area is increased in MCD and FSGS glomeruli.

Data are represented using box-and-whisker plots for cases before remission (BR; n=8) and after remission (AR; n=13) with MCD, subjects BR (n=8) and AR (n=10) with FSGS, and IgA-N cases (n=10). Results are analyzed using one way ANOVA. *: $p < 0.05$, and **: $p < 0.01$.

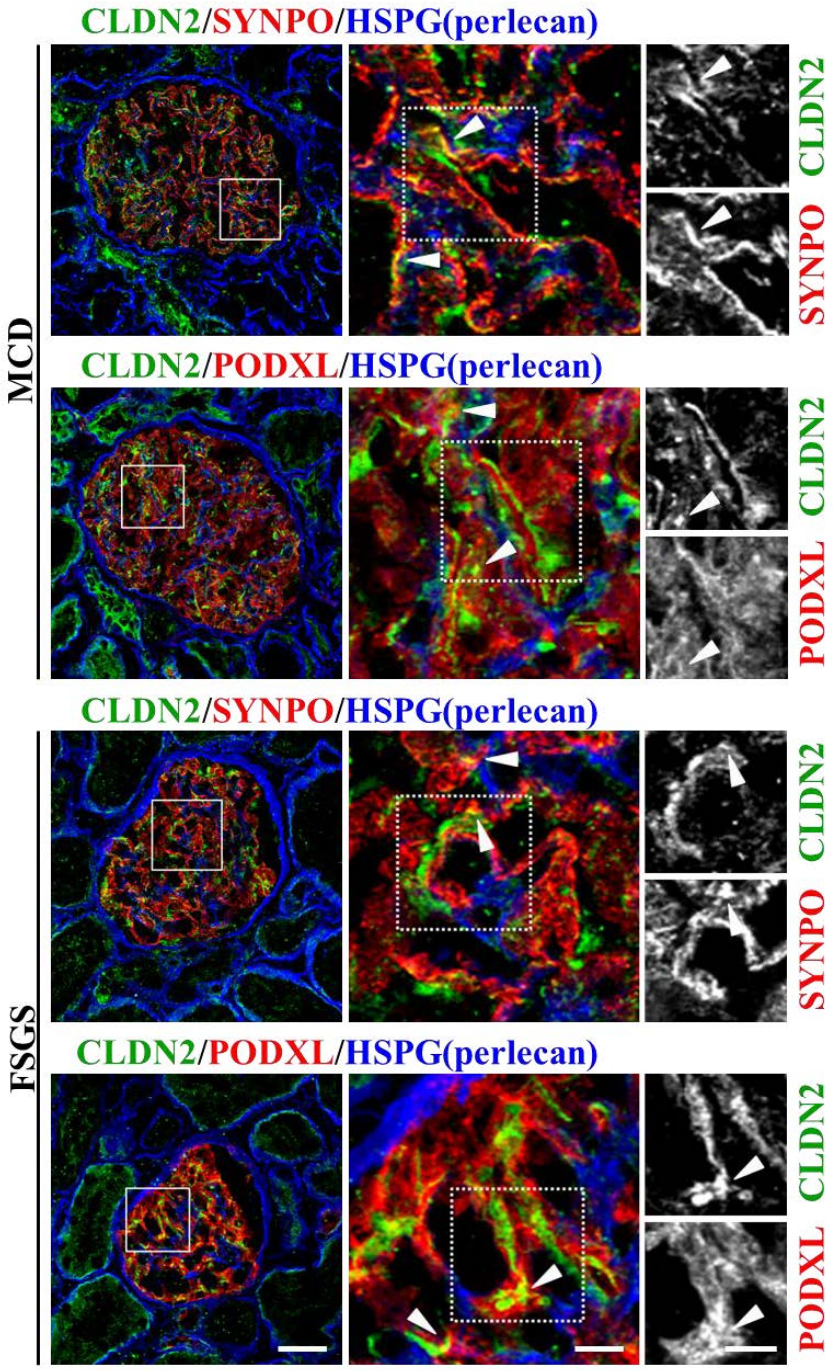

Figure 3: CLDN2 is at least partially colocalized with the podocyte markers synaptopodin (SYNPO) and podocalyxin (PODXL) in MCD and FSGS glomeruli before remission.

Renal biopsy sections were subjected to immunostaining with the corresponding antibodies. CLDN2 is stained green, SYNPO and PODXL are red, and HSPG (perlecan) is blue. Arrowheads indicate colocalization of CLDN2 with the podocyte markers. Bars; 50 μm in the left panel, 10 μm in the middle and right panels.

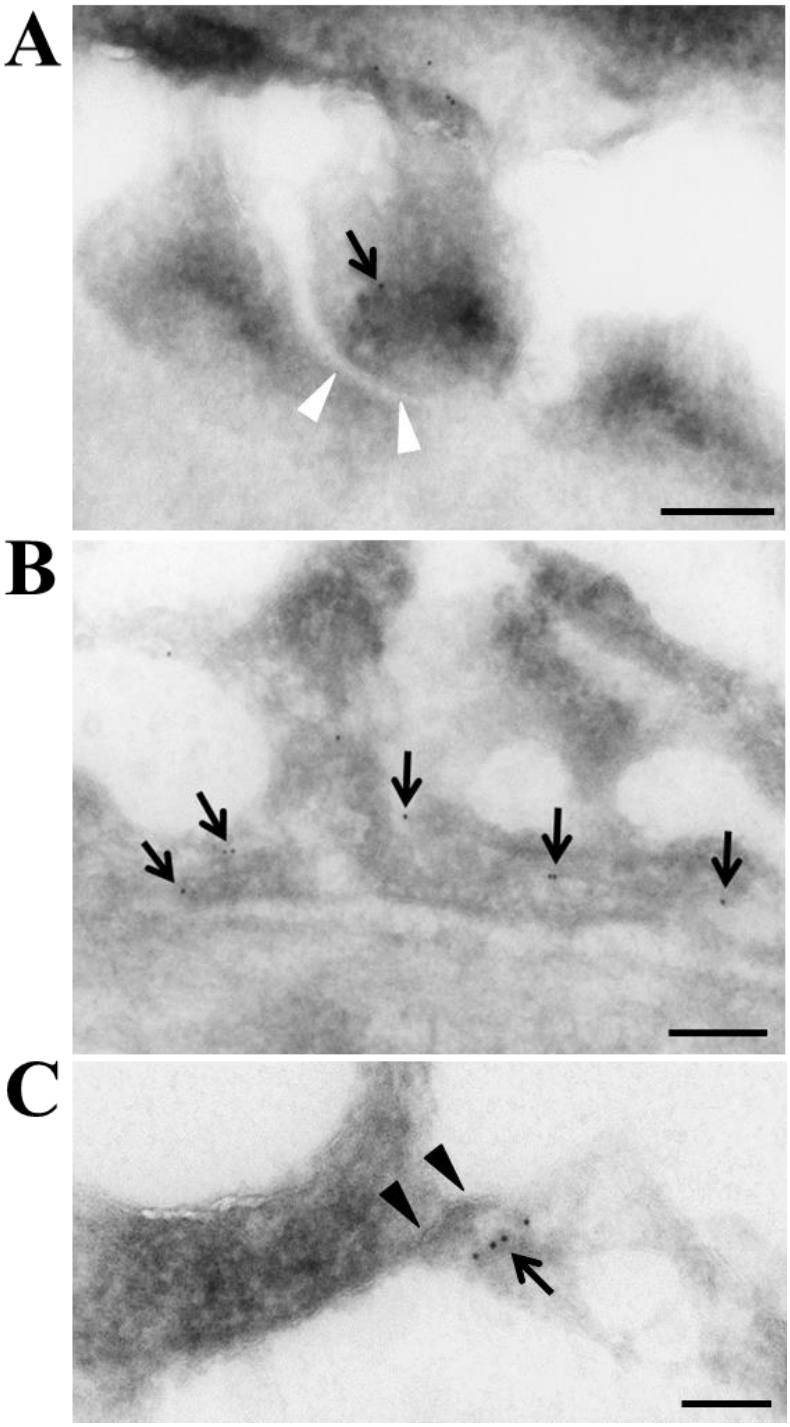

476

477 **Figure 4:** Immunogold electron micrographs showing the presence of CLDN2 in
478 podocytes from MCD before remission.
479 White and black arrowheads indicate SDs and newly formed TJs, respectively. Arrows
480 reveal the CLDN2 labeling in residual (A) and fused (B) foot processes, as well as at
481 TJs (C). Bars; 200 nm.

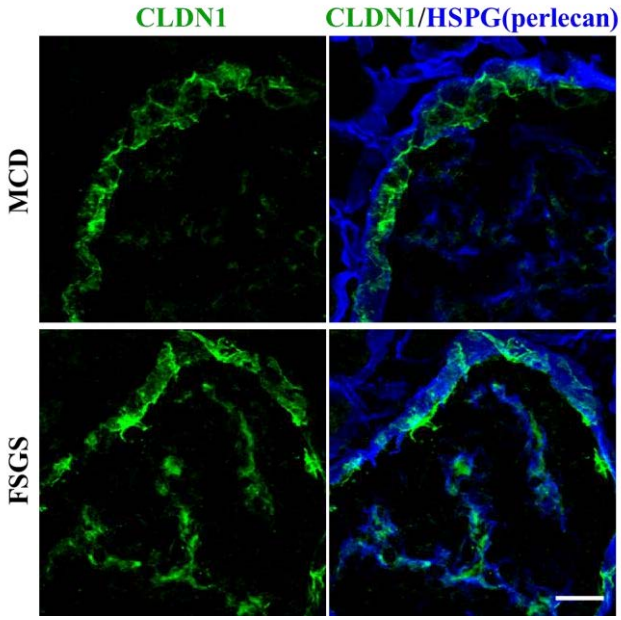

Figure 5: CLDN1 is segmentally observed in FSGS glomeruli but not in MCD glomeruli before remission.

Renal biopsy sections were subjected to immunostaining with the corresponding antibodies. CLDN1 is stained green and HSPG (perlecan) is blue. Bar, 25 μm.

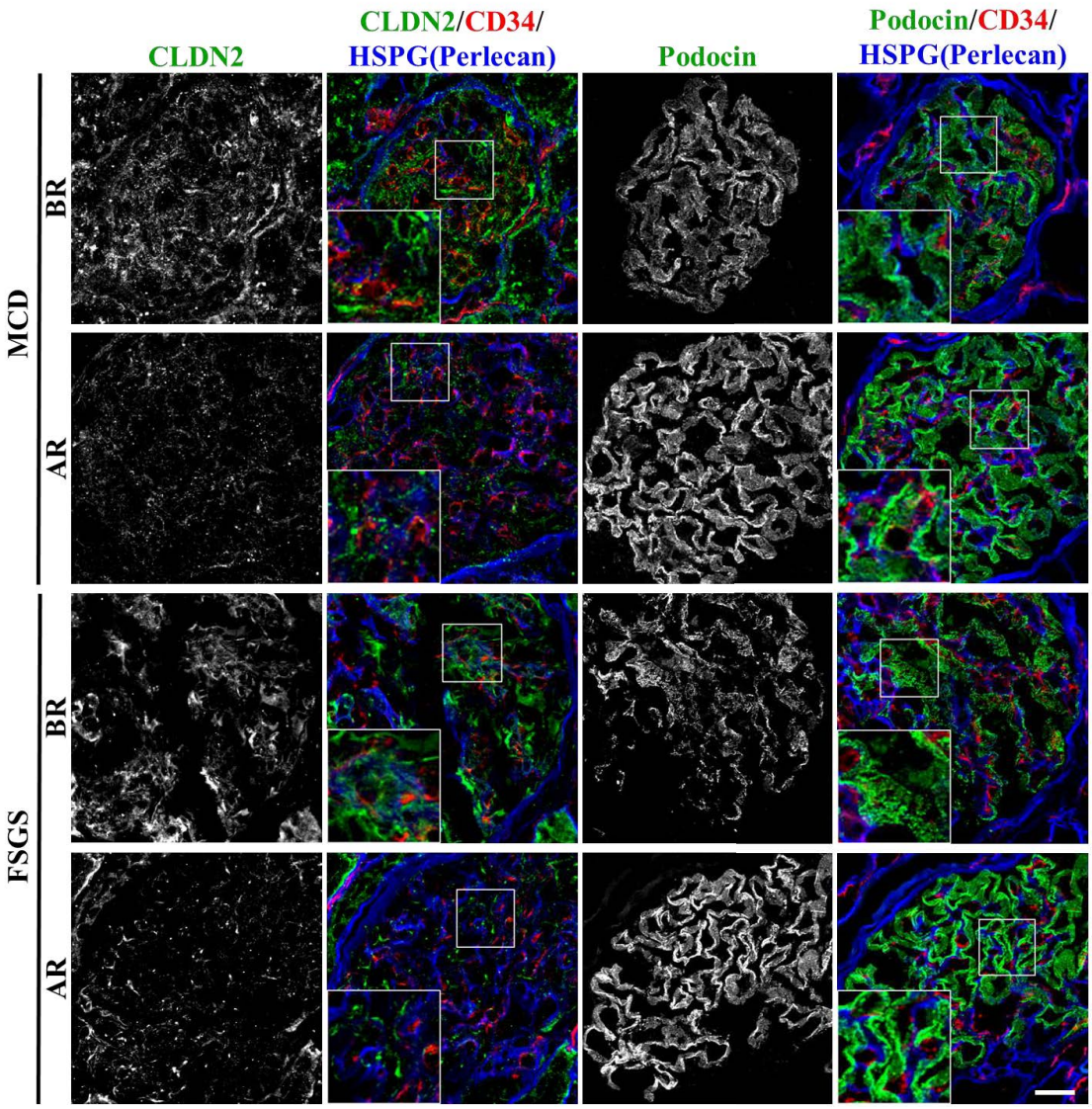

Figure 6: The strong filamentous signals for CLDN2 are appeared together with decrease of filamentous signals and change to the granulated pattern for podocin in MCD and FSGS glomeruli before remission.

Renal biopsy sections were subjected to immunostaining with the corresponding antibodies. Typical micrographs are shown for the before remission (BR) and after remission (AR) cases in MCD and FSGS. In the Merge panels, CLDN2 and podocin are stained green, CD34 is red and HSPG (perlecan) is blue. Bar, 25 μm.